A method for analyzing vibration power absorption density in human fingertip

John Z. Wu *, Ren G. Dong, Daniel E. Welcome, Xueyan S. Xu

National Institute for Occupational Safety and Health (NIOSH), 1095 Willowdale Road, Morgantown, WV 26505, USA

ARTICLE INFO

ABSTRACT

In the current study, we hypothesize that the vibration power absorption density (VPAD) is a good measure for the vibration exposure intensity of the soft tissues of the fingers. In order to calculate the VPAD at a fingertip, we proposed a hybrid modeling approach, which combines a 2D finite element (FE) model with a lumped parameter model. Whereas the lumped components are used to represent the global biodynamic characteristics of the hand-arm system, the FE component is used to predict the detailed stresses, strains, and VPAD in the fingertip. The lumped parameters are determined by using the vibration transmissibilities measured at the fingertip, while the material parameters of the soft and hard tissues of the FE model are adopted from the published experimental data. The proposed model was applied to predict the distributions of dynamic displacement, velocity, and VPAD in the soft tissues of the fingertip. Furthermore, we have derived the frequency weighting based on the VPAD of the soft tissue. The preliminary analysis indicated that the VPAD-based frequency weighting is substantially different from the ISO weighting in that the ISO frequency weighting emphasizes the effect of the vibration at frequencies lower than 25 Hz whereas the VPAD-based weighting generally emphasizes the resonant responses of the finger. Our analysis indicated that the VPAD-based weighting was fairly consistent with the finger surface vibration transmissibility at frequencies greater than the first resonance, suggesting that the finger surface transmissibility may be used as an alternative frequency weighting for assessing the finger vibration exposure. The proposed method provides a practical and efficient tool to simulate the detailed biodynamic responses of a complex biological system to vibration.

Published by Elsevier Ltd.

1. Introduction

Prolonged, intensive exposure to hand-transmitted vibration could cause a series of disorders in the sensorineural, vascular, and muscular systems of the fingers, which are the major components of hand-arm vibration syndrome [1,2]. It is well accepted that any effect of vibration exposure is generally frequency-dependent. However, a reasonable frequency weighting that accounts for many components of the vibration-induced finger disorders, such as the most studied vibration-induced white finger (VWF), has not been well established [3]. The current frequency weighting that has been conventionally used to assess the risk of the hand-arm vibration syndrome is specified in a consensus standard (ISO 5349-1) [4]. This weighting was formulated based on the subjective sensation of the entire hand-arm system

measured under some specific testing conditions [5]. Such a weighting may not truly reflect the frequency dependency of the vibration-induced finger disorders. Although a few epidemiological studies of the VWF have reported results consistent with the predictions of the standardized weighting method [6,7], many other studies have reported large discrepancies [8–15]. Therefore, the development of a more reasonable frequency weighting for assessing the risk of the vibration-induced finger disorders remains an important issue.

Naturally, the immediate biodynamic responses of the fingers can be best expressed as vibration-induced stress, strain, and power absorption in the finger tissues [16]. Such responses to mechanical stimuli incite the neural sensors of the fingers to detect the vibration and/or cause any injury to the finger soft tissues. It has also been well known that the mechanical stress and strain are essential factors that modulate the growth, remodeling, morphogenesis of the biological system [17]. Whereas many other factors may also influence the development of the vibration-induced finger disorders, the vibration-induced finger biodynamic responses might be the major factor that could cause physiological and subsequent pathological responses, which could eventually lead to the development of the finger disorders [1,16]. This concept is also supported from the observation that vibration-induced finger disorders are primarily associated with the local soft tissue [3], although vibration could also induce sympathetic responses of the fingers without direct exposure to vibration [1]. These observations suggest that there could be strong associations between the vibration-induced biodynamic responses and finger disorders, which further suggest that their frequency dependencies are at least partially related to each other. A comprehensive understanding of the biodynamic response weighting can help establish a better frequency weighting for risk assessment. More specifically, a preliminary frequency weighting can be derived from the finger biodynamic responses. The final weighting can be established by testing and revising the preliminary weighting through further physiological, pathological, and epidemiological studies. This may be a practical and effective approach to establish a more reasonable frequency weighting for assessing the risk of vibration-induced finger disorders.

Vibration power absorption density (VPAD) is a scalar parameter that combines the effects of tissue damping and vibration-induced stress and strain. We hypothesize that VPAD is a good measure for the vibration exposure intensity of the soft tissues of the fingers. Consistent with the concept of VPAD, several investigators proposed to use the vibration power absorption (VPA) to quantify the vibration exposure and hypothesized that VPA might be a significant etiological factor with regard to vibration-induced disorders [18–20]. Because it is technically difficult to quantify the VPA density, the total VPA of the entire hand-arm system was usually measured in previous studies. It was found that the frequency weighting derived from the total VPA was highly correlated with the ISO frequency weighting [21], suggesting that the total VPA is associated with the overall perception of the vibration and it is a measure similar to the ISO frequency-weighted acceleration. Thus, if the total VPA would be strongly associated with vibration-induced finger disorders, the current ISO weighting method would have provided a reasonable prediction of the VWF. As aforementioned, this does not seem to be the case. Whereas the total VPA may have some value for studying the vibration-induced disorders in the palm–wrist–arm–shoulder system, it may not be suitable for studying vibration-induced finger disorders [22].

Vibration-induced finger disorders are likely to be more closely associated with the VPAD in the fingers. To test this hypothesis, it is necessary to quantify the VPA or VPAD in the fingers. However, there is no practical method for direct evaluation of the VPA or VPAD in the fingers of a human subject. Alternatively, Dong et al. [23] proposed an approximate method to estimate the total VPA in the fingers using a mechanical-equivalent model of the finger–hand–arm system. Because the model does not include anatomical sub-structures of the fingers, it cannot be used to predict the VPA in the sections of a finger. In a separate study, an approximate method was proposed to predict the average VPAD of all the fingers [16]. Again, it is impossible to use such an approach to identify the distribution of the VPA or VPAD in each finger section, without taking into account the detailed anatomical structures of the hand-fingers in the modeling.

The current technology has made it possible to develop more comprehensive models of the fingers-hand-arm system for predicting more detailed distribution of the VPA and/or the VPAD in the soft tissues. Traditionally, there are two types of models simulating the responses of the human hand–arm system to vibration: lumped mass model and finite element (FE) model. In the lumped mass model, the hand–arm systems are represented using elements of spring, dashpots, and mass, and the global driving point biodynamics of the hand–arm–finger system can be simulated. Another approach is to use a FE method to mimic detailed anatomical structures of the biological system. Theoretically, the FE model can predict both applied-hand-force-induced and vibration-induced stresses, strains, and VPAD. However, it is technically demanding to model the entire hand–arm system using a FE method. In the current study, we propose a hybrid modeling method for analyzing the biodynamic responses of a fingertip, taking advantage of both modeling approaches. Whereas the lumped components will be used to represent the global biodynamic characteristics of the hand–arm system, the FE component will be used to predict the detailed stresses, strains, and VPAD in the fingertip. Using the proposed model, the methodology for deriving the frequency weighting based on the VPAD will be explored.

2. Method

2.1. Hand–finger model

The system of the hand–finger is simulated by using a lumped parameter model combined with a 2D FE model, as illustrated in Fig. 1A. The fingertip is simulated using a 2D finite element model, while the effective mass of the
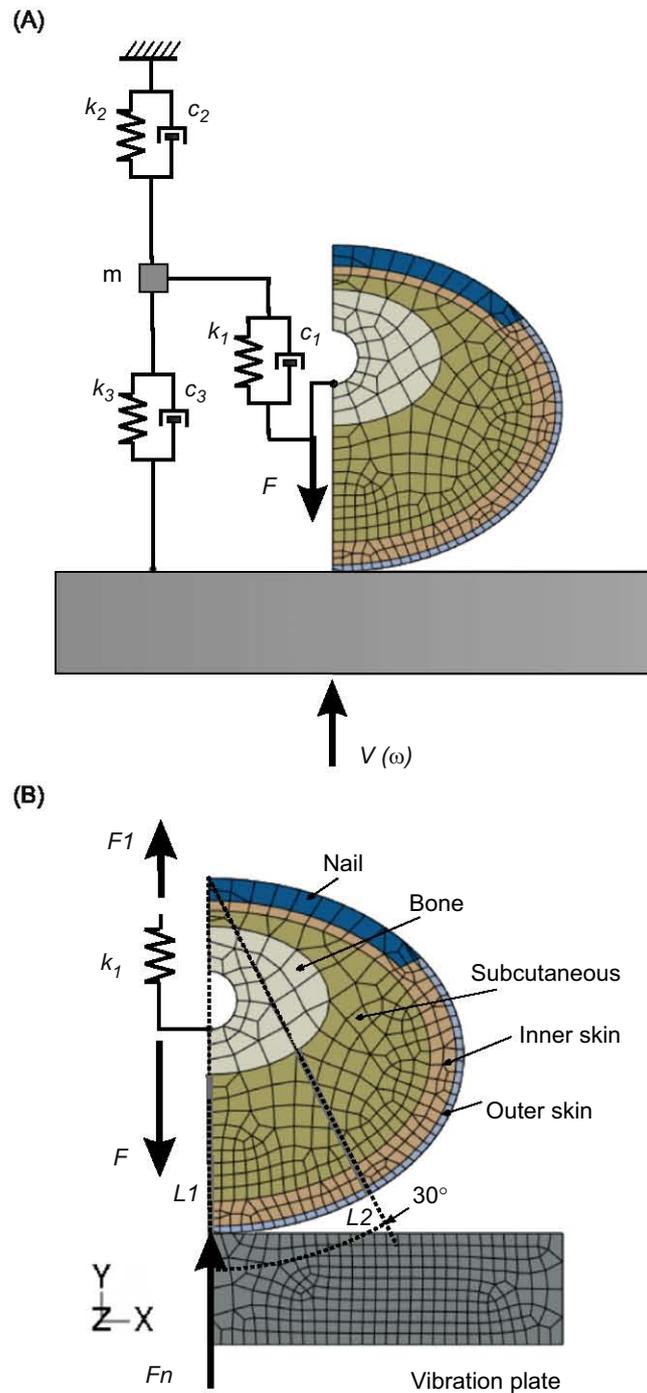
Fig. 1. Hybrid model of a fingertip. (A) The vibration response of the fingertip is simulated using a lumped parameter model combined with a 2D FE model. (B) Sketch for the calculation of the contact force between the force plate and the fingertip, *Fn*. The fingertip model includes nail, bone, outer skin, and inner skin, and subcutaneous tissues.

hand–finger is represented by the mass element *m*. The coupling between the fingertip and hand–finger is represented by the spring and damping element (k_1 and c_1). The contact between the fingertip and the vibrating plate is simulated in the FE modeling, while the coupling between the hand and the vibrating plate is represented by a spring/damping unit (k_3 and c_3). The coupling between the hand, forearm, and ground is represented by using another spring/damping unit (k_2 and c_2).

The fingertip model was assumed to be composed of skin layers, subcutaneous tissue, bone, and nail. The dimensions of the fingertip were determined based on the measurements of subject's finger and they are representative of the index finger of males [24,25]. The biquadral, plain-strain elements were used in the FE models and the commercial FE software package, ABAQUS (version 6.8), was utilized for the analyses. The nail is considered to have a thickness of 0.60 mm [26]. The skin is assumed to be composed of two layers: the outer skin (100 μm thick) and inner skin (1.26 mm thick). The outer skin layer contains stratum corneum (SC) and a part of the viable epidermis; and is considered as linearly elastic (Young's

Table 1
The parameters of the FE fingertip and the lumped parametric model used in the current simulations.

Materials	Mooney–Rivlin form			Elastic form		Density	Rayleigh	Damping
	C_{10} (MPa)	C_{01} (MPa)	D_1 (1/MPa)	E (MPa)	υ (–)	ρ (kg/m³)	α (1/s)	β (s)
Fingertip FE model								
Skin (outer)	*	*	*	2	0.3	1000	100	5.0E−06
Skin (inner)	2340	5420	2.0E−09	*	*	1000	100	5.0E−06
Subcutaneous tissue	597	1340	2.0E−09	*	*	1000	100	5.0E−06
Bone	*	*	*	10 000	0.3	2000	100	1.0E−08
Nail	*	*	*	170	0.3	2000	100	1.0E−08

Lumped parametric model							
m (g)	k_1^0 (N/m)	c_1^0 (N*s/m)	k_2^0 (N/m)	c_2^0 (N*s/m)	k_3^0 (N/m)	c_3^0 (N*s/m)
48	1937	2.57	562	16.00	13 273	18.53

modulus of 2 MPa and Poisson's ratio of 0.30); while the inner skin layer is composed of dermis and a part of the viable epidermis, and is characterized as nonlinearly elastic. The bone and nail are assumed to be linearly elastic [27], and have Poisson's ratio of 0.30 and Young's moduli of 17.0 GPa and 170.0 MPa, respectively. The two-term Mooney–Rivlin model is applied to characterize the nonlinearly elastic behaviors and the Rayleigh formula is applied for the frequency-dependent viscous damping characteristics of the soft tissues (i.e., the inner skin layer and subcutaneous tissues), as described in our previous studies [28,29]. The vibrating plate was assumed to have a thickness of 25 mm and a flat contact surface. The plate was considered to be made of aluminum with Young's modulus of 77.9 GPa and Poisson's ratio of 0.30. The parameters of the FE fingertip model are listed in Table 1.

2.2. Experimental procedure

Practically, the vibration transmissibility on the surface of a finger and/or the driving-point biodynamic response of the finger and hand can be directly measured. Each or both of them can be used to determine the remaining parameters of the model. In the current study, the vibration transmissibility of the fingertip was measured using a laser vibrometer (Polytec PSV-300-H). The basic measurement method and testing setup were similar to those reported in a previous study [30]. Briefly, a flat, rectangular aluminum platform (21.6 × 12.7 cm, 1.09 kg) connected to a single-axis vibration testing system (Unholtz-Dickie, TA250-S032-PB) was used to deliver the vibration, as shown in Fig. 2. The subject pushed against the plate with an open hand at four different given static force levels (from 15 to 30 N) during the measurement. The forearm of the subject was approximately horizontal and aligned with the wrist. The static and dynamic forces were measured using three force sensors (Kistler 9212), which connected the plate to the shaker. The remaining lumped parameters (m, c_i, and k_i, $i = 1, 2, 3$) were determined by fitting the predicted vibration transmissibility to the measured data using a least root-mean-square method [21]. The lumped parameters used in the simulations are listed in Table 1.

2.3. Numerical simulation procedure

The simulations were conducted using a displacement-controlled protocol in two stages. First, the fingertip was statically pre-compressed by applying a static force, F, at the bone center towards the contact plate. Second, the contact plate was subjected to a continuous harmonic vibration and the steady-state dynamic responses of the fingertip were analyzed using a linear perturbation procedure.

The contact force between the force plate and the fingertip, Fn, was calculated via a force equilibrium (Fig. 1B):

$$Fn = F - F1 = F - \Delta \cdot k_1 \tag{1}$$

where $F1$ and Δ is the force and deformation of the spring k_1, respectively.

The fingertip was assumed to undergo small harmonic vibrations around the deformed, stressed state, and the perturbed solutions were obtained using the tangential stiffness at the deformed state [31,32]. At the stressed state, the stiffness of the tissue is location-dependent due to the non-uniform deformation and the material nonlinearity. The perturbation procedure is linear—the contact area is assumed to be unchanged and the material properties are linearly viscoelastic. The dynamic analysis was performed in the frequency domain ranging from 16 to 1000 Hz.

2.4. Calculation of VPAD

The VPAD is defined as the vibration power absorption per unit volume of tissue. Assuming a tissue element with a volume, vol $= \Delta x \cdot \Delta y \cdot \Delta z$, is subjected to a sinusoidal vibration, u, under uniaxial force in the x direction, f_x, the VPA and

VPAD of the tissue element are derived conceptually:

$$VPA = \mathrm{Re}[f_x(\omega)\dot{u}(\omega)] \tag{2}$$

and

$$VPAD = \frac{VPA}{\mathrm{vol}} = \frac{VPA}{\Delta x \cdot \Delta y \cdot \Delta z} = \mathrm{Re}\left[\frac{f_x(\omega)}{\Delta y \cdot \Delta z} \cdot \frac{\dot{u}(\omega)}{\Delta x}\right]$$
$$= \mathrm{Re}[\sigma(\omega)\dot{\varepsilon}(\omega)] = \mathrm{Re}[\sigma(\omega)\varepsilon(\omega)\mathrm{j}]\omega \tag{3}$$

where $\mathrm{j} = \sqrt{-1}$; σ and ε is the stress and strain, respectively; and ω is the excitation frequency in rad/s.

Soft tissues are generally subjected to multi-axial loading, therefore, the contributions of the normal and shear stress/strain in all axes should be considered:

$$VPAD = \mathrm{Re}[\sigma_{ab}(\omega)\dot{\varepsilon}_{ab}(\omega)] = \mathrm{Re}[\sigma_{ab}(\omega)\varepsilon_{ab}(\omega)\mathrm{j}]\omega, \quad a,b = 1,2,3 \tag{4}$$

where σ_{ab}, ε_{ab}, and $\dot{\varepsilon}_{ab}$ is the tensor of the dynamic stress and strain, and strain rate, respectively.

For a linear system, both stress and strain are linearly proportional to the vibration magnitude, U, which is related to the input acceleration, A, by $U\omega^2 \propto A$. Therefore, it will be reasonable to assume that the VPAD is proportional to the square of the acceleration, A:

$$VPAD = \chi(\omega)A^2 \quad \mathrm{or} \quad \chi(\omega) = \frac{\mathrm{Re}[\sigma_{ab}(\omega)\varepsilon_{ab}(\omega)\mathrm{j}]\omega}{A^2} \tag{5}$$

where $\chi(\omega)$ is a parameter that is dependent on the stiffness and damping characteristics of the structure.

2.5. Frequency weighting derived from VPAD

The ISO frequency-weighted acceleration is proportional to the acceleration. To make the measurement of the VPAD directly comparable with the ISO weighted acceleration [21,22], VPAD is transformed into a form that is linearly proportional to the acceleration, A,

$$\sqrt{VPAD} = \sqrt{\chi(\omega)}A \tag{6}$$

This expression indicates that the frequency weighting based on the VPAD should be dependent on $\sqrt{\chi(\omega)}$. After normalization with respect to its maximum value and the maximum value (0.958) of the ISO frequency weighting in the one-third octave bands, the VPAD-based frequency weighting can be expressed as

$$W_{VPAD}(\omega) = 0.958 \frac{\sqrt{\chi(\omega)}}{\mathrm{Max}\sqrt{\chi(\omega_{\mathrm{ref}})}} = 0.958 \frac{\sqrt{\mathrm{Re}[\sigma_{ab}(\omega)\varepsilon_{ab}(\omega)\mathrm{j}]\omega}/A}{\mathrm{Max}\sqrt{\chi(\omega_{\mathrm{ref}})}} \tag{7}$$

where ω_{ref} is the reference frequency, at which the variable $\chi(\omega)$ reaches its maximum. Consequently, the frequency weighting function, $W_{VPAD}(\omega)$, is dimensionless and has a maximum value of 0.958.

The VPAD-based frequency weighting, as expressed in Eq. (7), is in the same scale as the frequency weighting of ISO and both weighting curves are directly comparable.
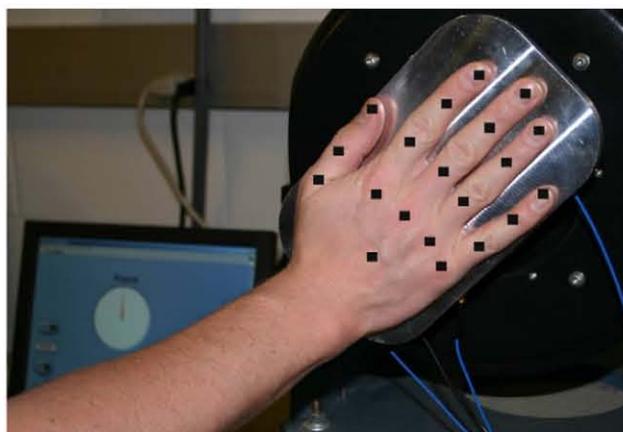

Fig. 2. Set-up for testing vibration transmissibility of human hand–finger system. A constant-velocity (8 mm/s) broad-band random vibration from 16 to 1250 Hz was used as the excitation. The black squares in the picture represent the scanning spots of the laser vibrometer.

3. Results

3.1. Deformations of the fingertip under static loading

The applied force at the bone center, F, and the contact force between the fingertip and vibration plate, Fn, as a function of the fingertip deformation are depicted in Fig. 3. The fingertip deformation is defined as the displacement difference between the bone center and the contact surface. The 2D FE model is considered to have a thickness of 10 mm, therefore, the forces are expressed in terms of N/cm. It is seen that F is almost linearly related to the fingertip deformation, whereas the relationship between Fn and fingertip deformation is nonlinear. That is because only a small portion of the applied force contributed to the fingertip deformation, and most of the applied force is carried out by the other part of the hand.

For four representative contact force levels, $F1$ (= 0.1 N/cm), $F2=2F1$, $F3=3F1$, and $F4=4F1$, we calculated the distributions of the static deformations in the fingertip, as shown in Fig. 4. The left and right columns of the figure show the horizontal and vertical displacements (shown as $U1$ and $U2$ in figure), respectively.

3.2. Model calibration

By adjusting the lumped parameters (k_i and c_i, i=1, 2, 3, and m), the model predictions on the magnitudes of the vibration transmissibility are fitted to the experimental data, as shown in Fig. 5. The transmissibility is defined as the ratio of the vibration magnitude at the nail to that at the vibration plate. Both numerical and physical tests were conducted at the same constant vibration velocity of 8 mm/s. It is seen that the model predictions for the first and second resonant responses agree well with the experimental measurements. The comparison of the corresponding phase variations between the theoretical predictions and the experimental data is shown in Fig. 6. It is seen that the theoretically predicted phase angles agree in trend with the experimental data for vibration frequencies lower than 100 Hz. The lumped parameters of the model were found to be dependent on the static compression:

$$c_i = c_i^0 \cdot c_{\text{damp}}, \quad k_i = k_i^0 \cdot k_{\text{damp}} \tag{8}$$

where c_i^0 and k_i^0 are the damping coefficient and spring stiffness at the reference level (Table 1), respectively; and c_{damp} and k_{damp} are functions of the static compression, as illustrated in Fig. 7.
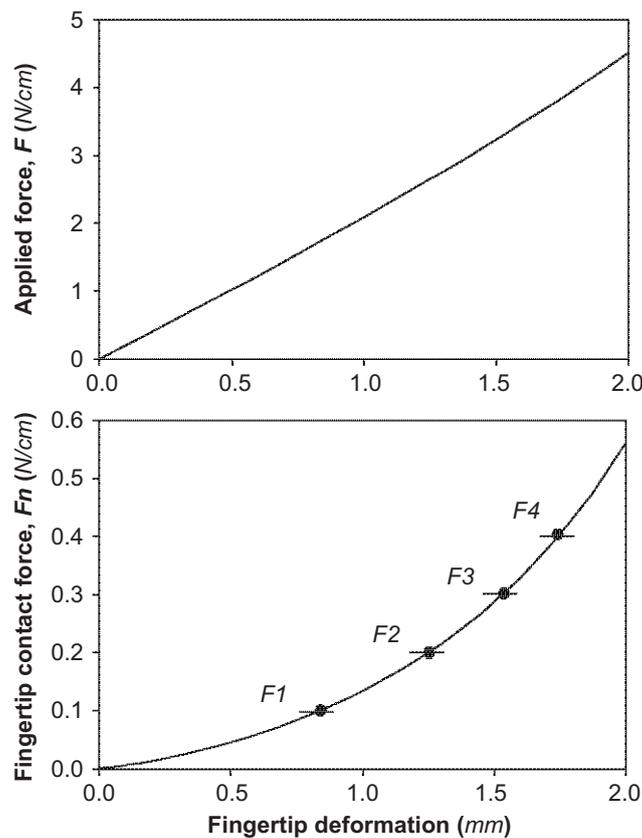

Fig. 3. Total applied force and the fingertip contact force as a function of the fingertip deformation. The fingertip deformation is defined as the difference in the vertical displacement between the contact surface and the bone center.
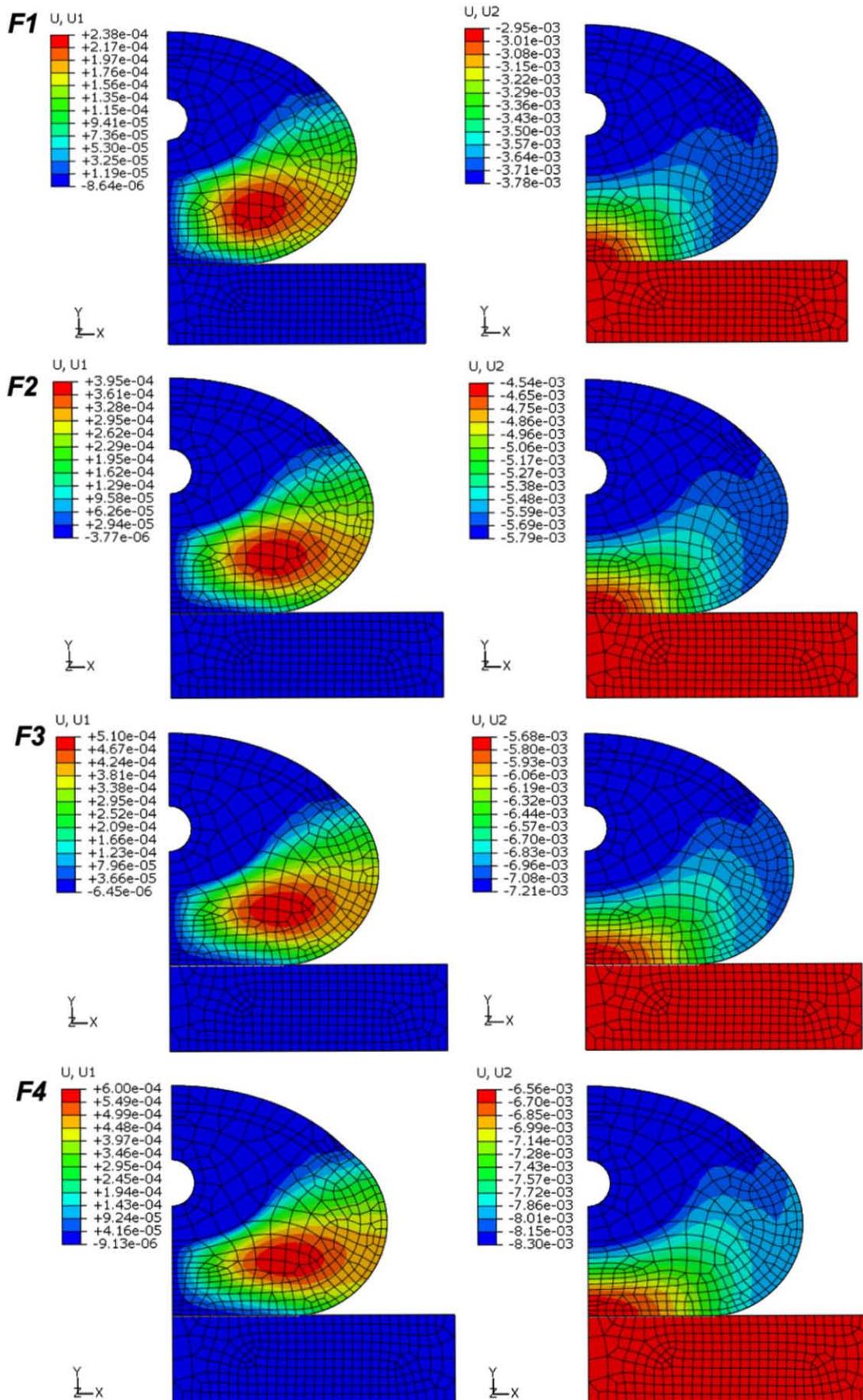
Fig. 4. The distributions of the horizontal (*U*1, left column) and vertical displacement (*U*2, right column) of the fingertip subjected to different pre-compression forces. A section thickness of 1 cm in the 2D model is considered, such that $F1=0.1$ N, $F2=2F1$, $F3=3F1$, $F4=4F1$. *U*1 and *U*2 are in mm.
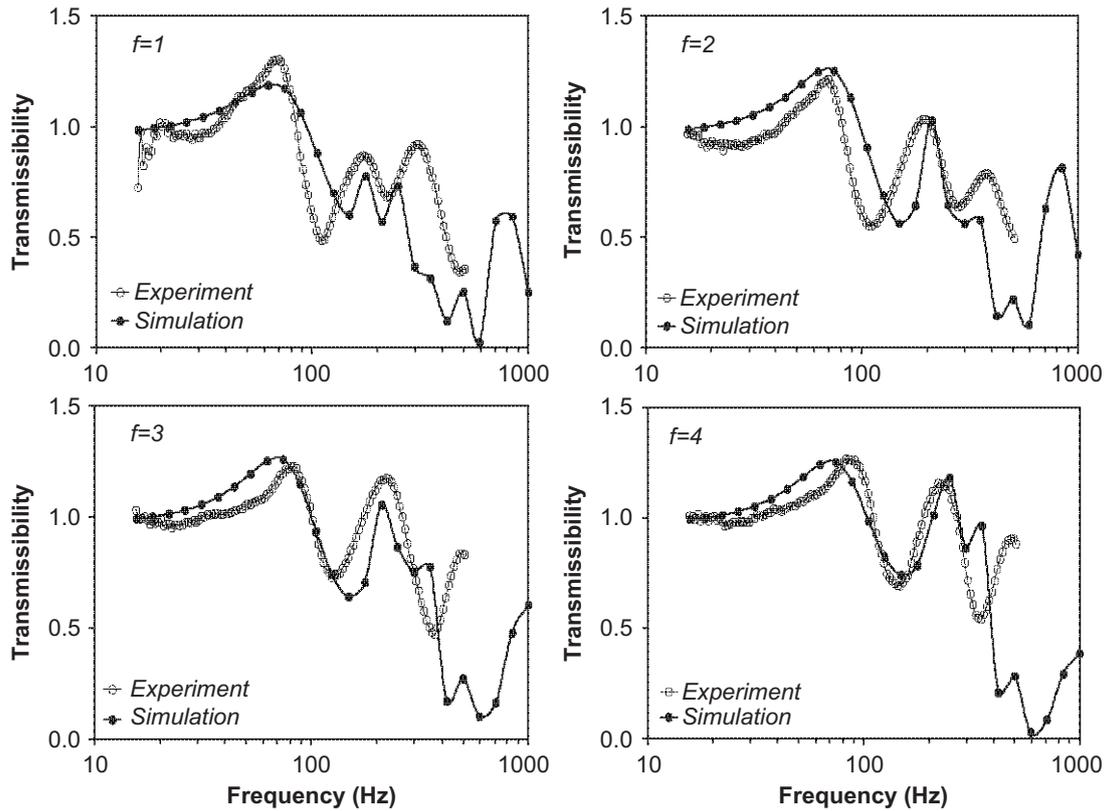
Fig. 5. Comparison of the simulated vibration transmissibility (•) at the fingertip with the experimental data (○). Four different pre-compression forces were applied to the fingertip, before the fingertip was subjected to vibration. The normalized force is defined as: $f=Fi/F1$ (i=1,2,3,4), with $F1$=0.1 N, $F2$=2$F1$, $F3$=3$F1$, and $F4$=4$F1$.

3.3. Effects of the static contact force and tissue damping

The transmissibility of the vibration at the fingertip and the corresponding phase shifts as a function of the static pre-compression is shown in Fig. 8. In this series of numerical tests, the normalized static compression force ($f=Fi/F1$, i=1,2,3,4) is increased one, two, and three times from f=1, while all other model parameters were kept unchanged. The results show that the first and the second resonant frequencies of the fingertip are around 70-80 Hz and around 200 Hz, respectively. The static compression has an effect on the vibration magnitude, but no effect on the resonant frequency.

The simulation results for the effects of the tissue damping on the transmissibility and the phase shift are shown in Fig. 9. In this series of numerical tests, the tissue damping factor was increased from $0.5\beta_0$ ($\beta_0 = 5 \times 10^{-6}$ s) to β_0, $2\beta_0$, and $4\beta_0$, while the other parameters were unchanged. It is seen that the vibration transmissibility magnitudes around the resonances are reduced with increasing tissue damping, and that tissue damping has little effect on the phase angle variations. Again, the resonant frequency is not affected by the variations of the tissue damping.

3.4. Distributions of dynamic displacement, velocity, and VPAD in the soft tissues

The representative results for the frequency-dependent distributions of the vibration displacement magnitude across the fingertip are shown in Fig. 10. Since the numerical tests were conducted under constant vibration velocity at the contact plate (8 mm/s), the magnitude of the maximal displacement magnitude decreases with increasing frequency, as expected.

Fig. 11 shows the results of the distributions of the vibration velocity magnitude across the fingertip sections. It is seen that velocity magnitude of the plate is constant (8 mm/s), while the penetration of the vibration into the soft tissues is frequency-dependent. Although the undeformed shapes of the fingertip model are shown in these figures for the purpose of illustrating, the fingertip is, in fact, vibrated under a pre-compressed state.

The distributions of vibration magnitude, velocity, and VPAD along the central line of the fingertip model are depicted in Fig. 12. The spatial distances of the plots refer to the fingertip in the undeformed state. The distributions of these parameters within the soft tissues are of major concern (i.e., the range from the bone/soft tissue interface to the tissue/plate contact interface). The frequency-dependent characteristics of the vibration penetrations into the soft tissues are quantitatively analyzed in these figures. At the tissue/plate contact surface, the vibration velocity is constant at 8 mm/s (Fig. 12B) and the corresponding vibration magnitude decreases with increasing frequency (Fig. 12A). However, the
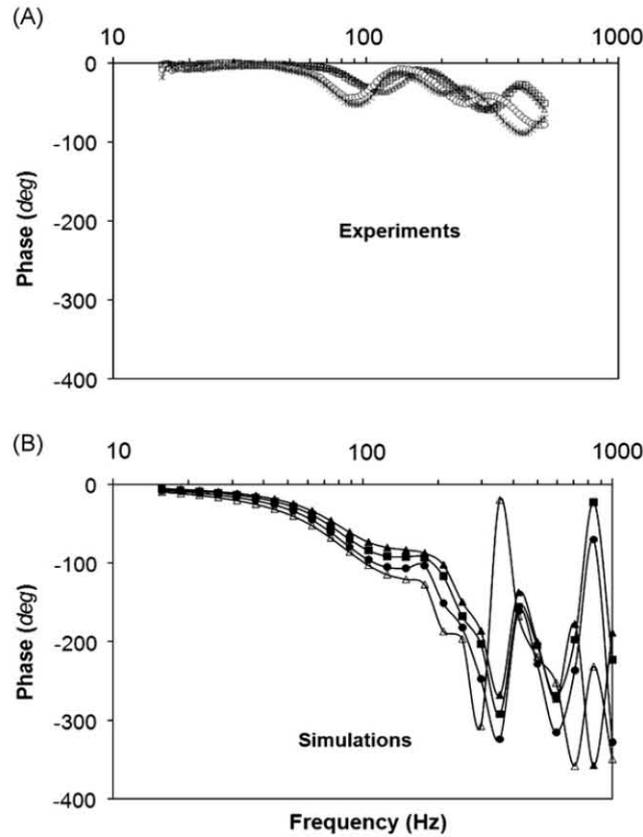
Fig. 6. Comparison of the simulated phase change of the vibration transmissibility at the fingertip with the experimental data. The fingertip was pre-compressed by four different forces before subjected to vibration. (A) Experiments (*: $f=1$; ○: $f=2$; □: $f=2$; △: $f=4$). (B) Simulations (△: $f=1$; ●: $f=2$; ■: $f=3$; ▲: $f=4$). The normalized force is defined as: $f=Fi/F1$ ($i=1,2,3,4$), with $F1=0.1$ N, $F2=2F1$, $F3=3F1$, and $F4=4F1$.
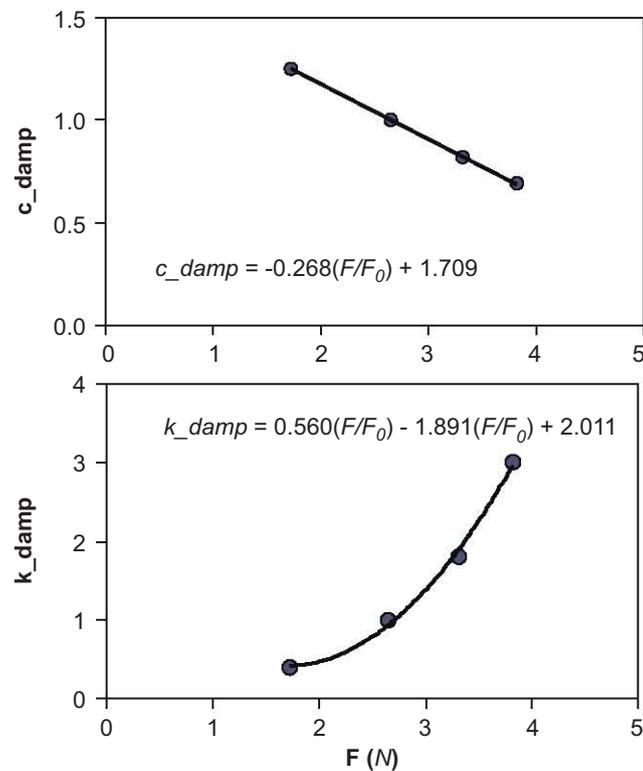

Fig. 7. The variation of the stiffness and damping parameters of the lumped elements as a function of the applied pre-compression force. (A) Damping parameter, $c_{damp} = -0.268\,(F/F_0)+1.709$. (B) Stiffness parameter, $k_{damp}=0.560(F/F_0)^2-1.891(F/F_0)+2.011$. F is in N, and $F_0 = 1$ N.
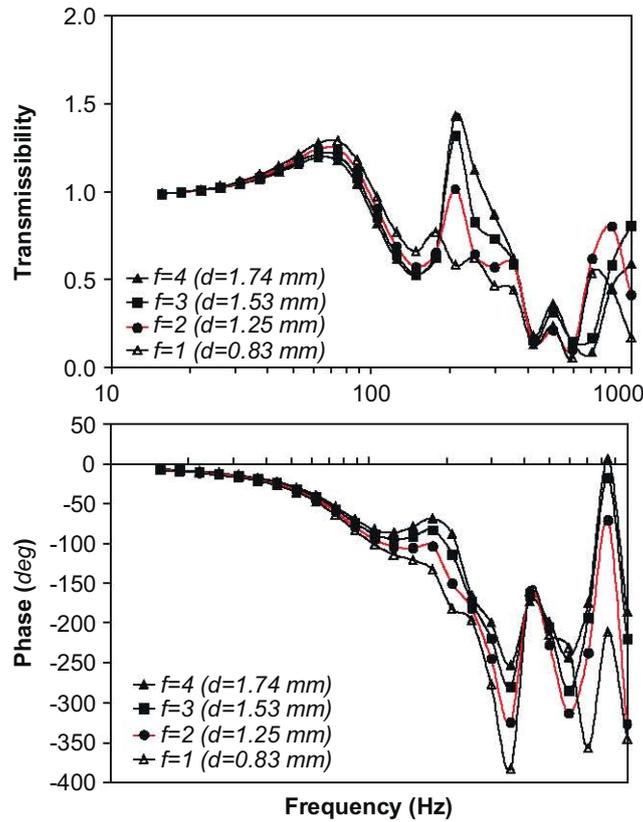
Fig. 8. The effects of the pre-compression forces on the vibration transmissibility of the fingertip. The fingertip was pre-compressed by different forces before subjected to vibrations. △: $f=1$ ($d=0.83$ mm); •: $f=2$ ($d=1.25$ mm); ■: $f=3$ ($d=1.53$ mm); and ▲: $f=4$ ($d=1.74$ mm). The normalized force is defined as: $f=Fi/F1$ ($i=1,2,3,4$), with $F1=0.1$ N, $F2=2F1$, $F3=3F1$, and $F4=4F1$.
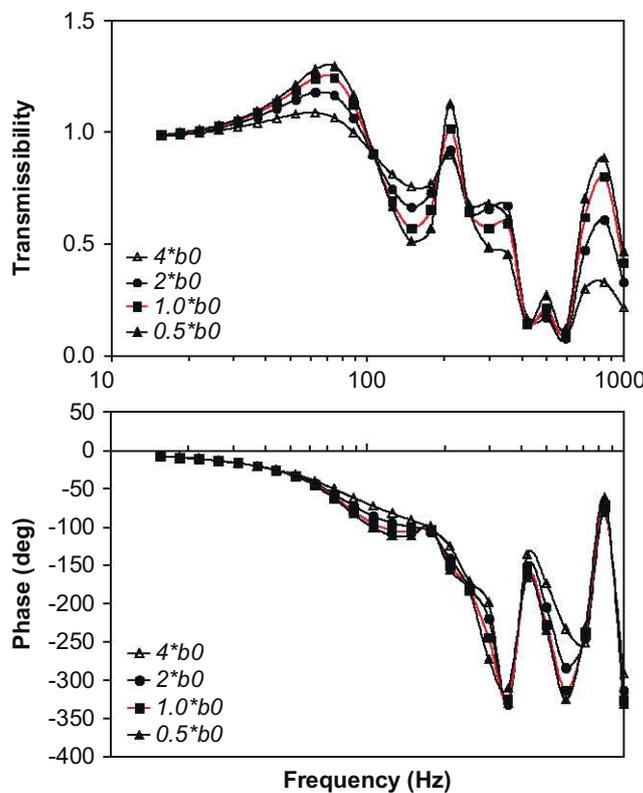

Fig. 9. The effects of the tissue damping on the vibration transmissibility of the fingertip. The tissue damping is reduced by 50%, or increased by 100% and 300%. The pre-compression force is unchanged at $F2=0.2$ N for the simulations. ▲: $0.5\beta_0$; ■: $1.0\beta_0$; •: $2.0\beta_0$; △: $4.0\beta_0$, with $\beta_0 = 5 \times 10^{-6}$ s.
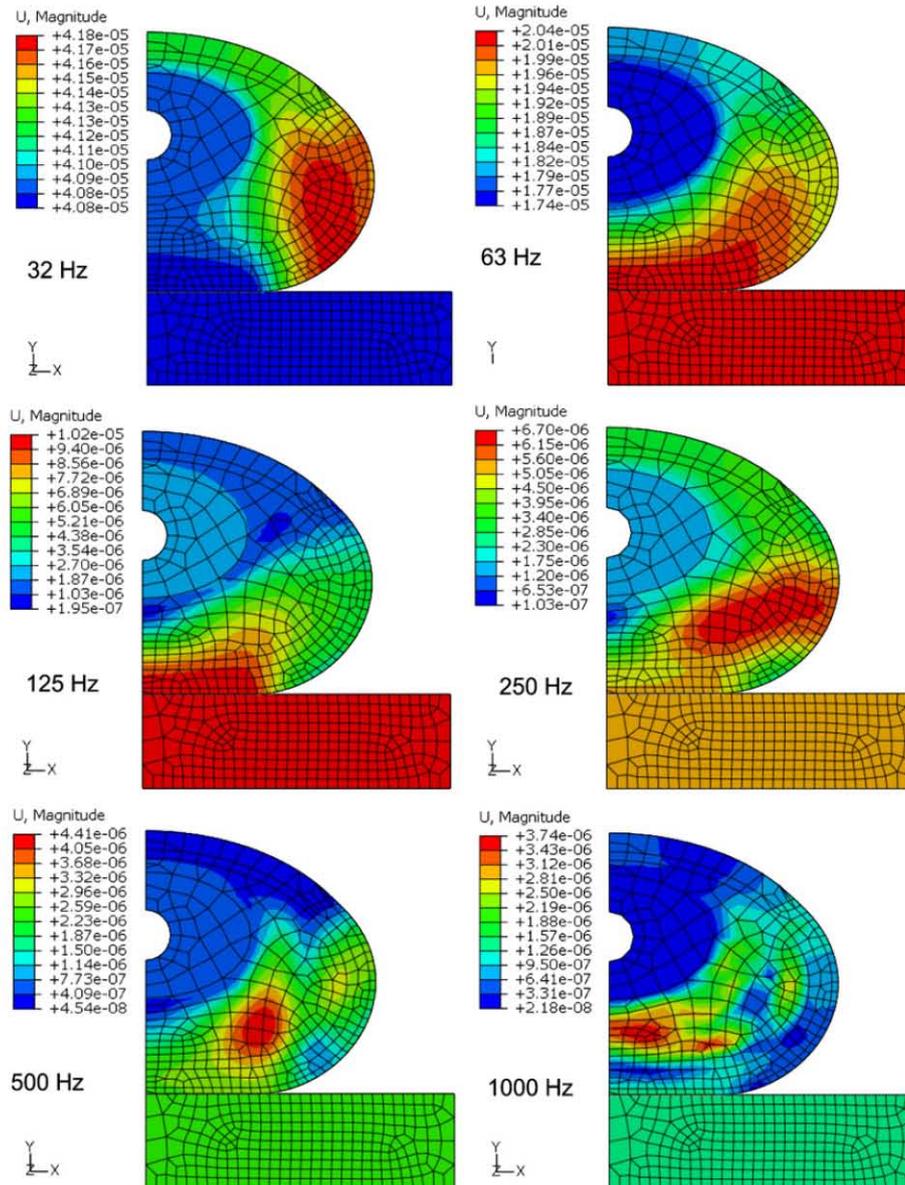
Fig. 10. The distributions of the dynamic displacement magnitude (*U*) of the fingertip as a function of vibration frequency. *U* is in mm.

distributions of the vibration within the soft tissue depend on the frequency; especially when the frequency is equal to or greater than 125 Hz, the distribution patterns of the vibration in the soft tissue varied suddenly: the gradients of vibration displacement and velocity across the tissue become substantially greater.

3.5. VPAD-based frequency weighting

Using the results of the VPAD distributions (Fig. 12C), the VPAD-based frequency weighting curves are calculated using Eq. (7), as shown in Fig. 13A and B. Each of the VPAD-based weighting curves was derived using the VPAD data at one point in the soft tissue along the centerline (*L* 1) and along a line 30° from the center line (*L* 2), as illustrated in Fig. 1B. The location of the points within the tissue is described by a normalized scale, *s/L*, along the lines; *s/L*=0 and 1.0 represent the bone/tissue interface and the skin surface, respectively. The points at the bone/tissue interface (*s/L*=0) and the tissue/plate contact interface (*s/L*=1 on line *L* 1) were not considered, because they contain artifacts in the interfaces. The curves of the ISO frequency weighting and the normalized vibration transmissibility at the nail are also shown in the figure for comparison.

4. Discussion and conclusion

In the current study, we proposed to simulate the vibration of the human arm–hand–finger system using a hybrid model that combines a finite element model of a fingertip with a lumped parameter model of the hand–arm system.
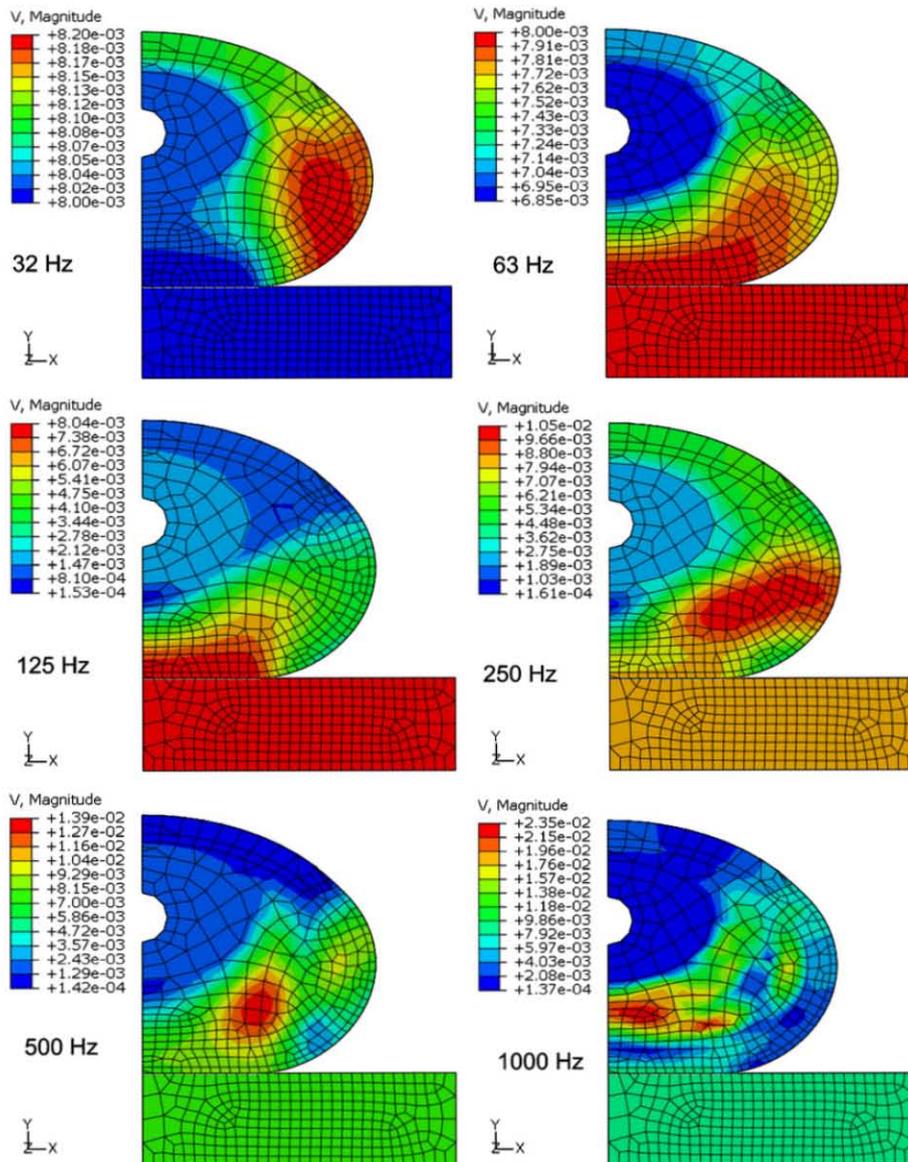
Fig. 11. The distributions of the dynamic velocity magnitude (*V*) of the fingertip as a function of vibration frequency. *V* is in m/s.

We demonstrated in the study that the proposed modeling approach can effectively take into account both local and global responses, such that the vibration-induced tissue stress, strain, and power absorption density in the fingertip, as well as the global driving point biodynamics can be predicted. The static stress and strain due to the static compression of the fingertip can also be predicted using this model. Although only the fingertip biodynamic responses were simulated in the current study, such a modeling approach can be generalized to predict the detailed biodynamic responses of other anatomical substructures of the hand–arm system. The proposed method is a practical and efficient approach to simulate the detailed biodynamic responses of a complex biological system in vibration.

The fingertip can be subjected to different static compressions in operating a vibrating tool or machine. The contact stiffness of a fingertip is nonlinear, as illustrated in the current simulations (Fig. 3). Because of the nonlinearity of the materials, the stiffness of the soft tissues varies with the status of the static deformation. The static pre-compression influences the stiffness of the soft tissues differently in different locations within the tissues. The vibration responses of the soft tissues vary due to the change of the tissue stiffness caused by the pre-compression. The pre-compression of the fingertip is thus coupled with the vibration transmissibility or biodynamic responses. All these phenomena are described by the proposed model (Figs. 6–8).

As anticipated, the biodynamic responses of the fingertip and their modal patterns are generally frequency-dependent, as shown in Figs. 10 and 11. One of the factors that contributes to the frequency-dependent responses of the fingertip is the tissue damping. Whereas it is extremely difficult to accurately measure the tissue damping, we performed a parametric study to explore its influence. The simulation results suggest that the tissue damping property could effectively affect the
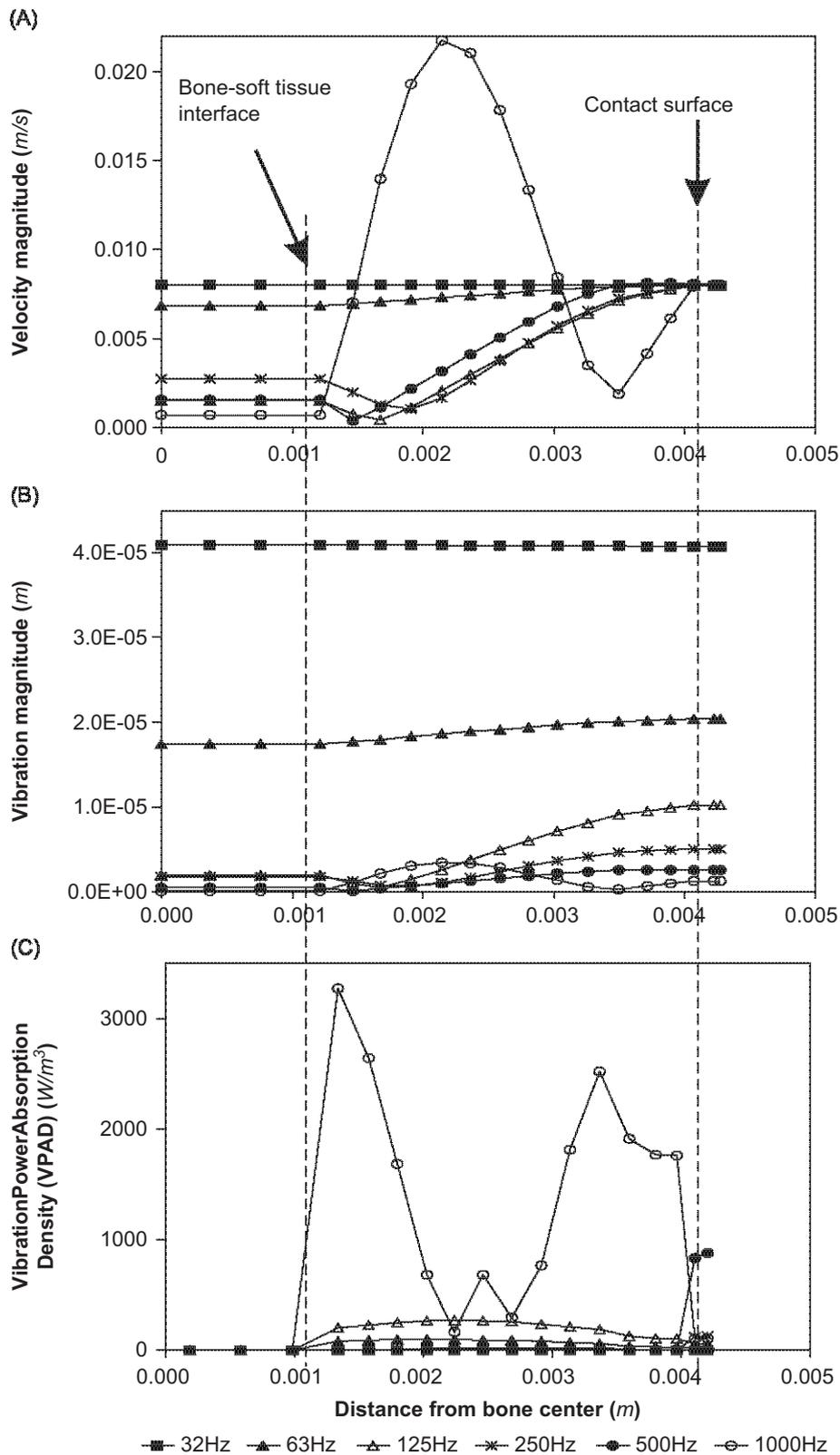
Fig. 12. The distributions of vibration magnitude, velocity, and VPAD along the central line of the fingertip model. The spatial distance of the plots is referred to the fingertip at the un-deformed state.

magnitudes of the biodynamic responses, but would have little influence on the frequency dependency of the responses, as shown in Fig. 9.

Under the specific testing conditions used in this study, the first resonance observed in the vibration transmissibility was in the range from 60 to 90 Hz, as shown in (Fig. 5). The first resonance is usually greatly influenced by the global
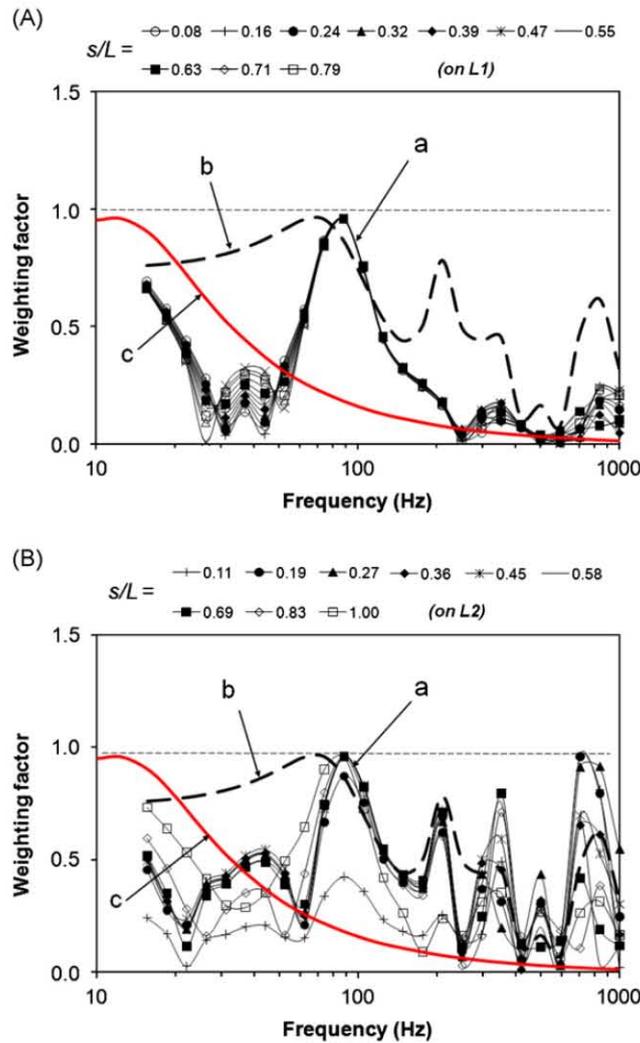
Fig. 13. The comparison of the frequency weighting derived using VPAD with ISO-weighting and the weighting derived using the finger surface vibration transmissibility. (A) Calculated along line L 1. (B) Calculated along line L 2. Each of these weighting curves based on VPAD is derived using the data at one point in the soft tissue along line L 1 (A) and line L 2 (B). L 1 and L 2 represents the centerline and a line 30° from the centerline, respectively, as illustrated in Fig. 1B. The value of s/L represents the position in the soft tissue: 0 for the bone/tissue interface, and 1.0 for the skin surface. a: VPAD-based weighting, b: transmissibility-based weighting, and c: ISO weighting.

response of the entire hand-arm system [16]. Therefore, it is necessary to take into account the global response in the simulation of any substructure of the hand-arm system. This was considered in the proposed model.

The second major resonance was in the range between 160 and 250 Hz (Fig. 5). The vibration distribution patterns reported by [30] indicate that this resonance is primarily associated with the local fingertip response. This is consistent with the experimental observation that the high frequency response of the fingers is not significantly influenced by the other part of the hand–arm system [21]. There are a few resonances at higher frequencies. They are more localized resonances and some of them are also reflected in the frequency weightings presented in Fig. 13.

The distributions of the vibration magnitude and velocity varied suddenly between frequencies 63 and 125 Hz: they are more uniformly distributed across the tissues for frequencies less than 63 Hz, while the gradient across the tissues increased suddenly for frequencies higher than 125 Hz (Fig. 12A and B), which also indicates that the responses at higher frequencies become more localized.

Because of the frequency-dependent distributions of the stress/strain in the soft tissues, the VPAD-based weighting depends on the reference location in the tissue. In this study, we calculated the VPAD-based weighting only on points along two lines with the tissues. As shown in Fig. 13B, the transmissibility curves are similar to the outline profile of the VPAD-based weighting curves. This suggests that the finger surface vibration transmissibility at frequencies higher than the first resonance could be approximately utilized to represent the weighting of the biodynamic response. It is technically less challenging to derive a frequency weighting based on the finger vibration transmissibility because the transmissibility on the surface of each finger can be directly measured using a laser vibrometer.

The VPAD-based frequency weighting is substantially different from the ISO weighting, as shown in Fig. 13. Obviously, the ISO frequency weighting emphasizes the effect of the vibration at frequencies lower than 25 Hz. The VPAD-based

weighting emphasizes the biodynamic response close to the resonance frequency observed in the finger vibration transmissibility.

It is noted that the fingertip resonance frequencies identified in this study may not be generally applied. This is because the resonance frequencies depend on many factors such as handle geometry, hand–tool coupling conditions, vibration direction, and applied hand forces. For example, the first resonance frequency in a power grip on a cylindrical handle along the forearm direction is usually in the range from 20 to 60 Hz [21], which is different from that observed in the current study with an open hand pushing on a flat plate. The resonance frequencies could also be individual-specific. However, the proposed modeling approach can be used to determine more generally applicable VPAD-based frequency weighting when more data of experimental measurements of the finger vibration transmissibility and/or finger driving-point biodynamic response become available.

Disclaimers

The findings and conclusions in this report are those of the authors and do not necessarily represent the views of the National Institute for Occupational Safety and Health.

References

[1] M.J. Griffin, *Handbook of Human Vibration*, Academic Press, San Diego, London, 1990.
[2] P.L. Pelmear, D.E. Wasserman, *Hand–Arm Vibration: A Comprehensive guide for Occupational Health Professionals*, second ed., OEM Press, Beverly Farms, Massachusetts, 1998.
[3] M. Bovenzi, Vibration-induced white finger and cold response of digital arterial vessels in occupational groups with various patterns of exposure to hand-transmitted vibration, *Scandinavian Journal of Work, Environment & Health* 24 (2) (1998) 138–144.
[4] ISO-5349, Mechanical vibration—measurement and assessment of human exposure to hand-transmitted vibration—part 1: general guidelines, International Organization for Standard (ISO), 5349, 2001.
[5] T. Miwa, Evaluation methods for vibration effect. Part 3: measurement of thresholds and equal sensation contours on hand for vertical and horizontal sinusoidal vibrations, *Industrial Health* 5 (1967) 213–220.
[6] A. Brammer, W. Taylor, J. Piercy, Assessing the severity of the neurological component of the hand–arm vibration syndrome, *Scandinavian Journal of Work, Environment & Health* 12 (4 Spec No) (1986) 428–431.
[7] H. Anttonen, H. Virokannas, Hand vibration among snowmobile drivers and prediction of vwf by vibration standard, in: H. Dupuis, E. Christ, J. Sandover (Eds.), *Proceedings of the 6th International Conference on Hand-Arm Vibration*, , 1992, pp. 875–883.
[8] R. Dandanell, K. Engstrom, Vibration from riveting tools in the frequency range 6 Hz–10 Mhz and raynaud's phenomenon, *Scandinavian Journal or Work, Environment & Health* (1986) 338–342.
[9] M. Bovenzi, Vibration white finger, digital blood pressure, and some biochemical findings on workers operating vibrating tools in the engine manufacturing industry, *American Journal of Industrial Medicine* 14 (5) (1988) 575–584.
[10] T. Nilsson, L. Burstrom, M. Hagberg, Risk assessment of vibration exposure and white fingers among platers, *International Archives of Occupational & Environmental Health* 61 (7) (1989) 473–481.
[11] P.L. Pelmear, D. Leong, W. Taylor, M. Nagalingam, D. Fung, Measurement of vibration of hand-held tools: weighted or unweighted?, *Journal of Occupational Medicine* 31 (11) (1989) 902–908
[12] R. Lundstrom, A. Lindmark, Effects of local vibration on tactile perception in the hands of dentists, *Journal of Low Frequency Noise, Vibration* 1 (1) (1982) 1–11.
[13] M. Griffin, M. Bovenzi, C. Nelson, Dose-response patterns for vibration-induced white finger, *Occupational and Environmental Medicine* 60 (2003) 16–26.
[14] J. Starck, P. Jussi, P. Ilmari, Physical characteristics of vibration in relation to vibration-induced white finger, *American Industrial Hygiene Association Journal* 51 (4) (1990) 179–184.
[15] M. Bovenzi, A prospective cohort study of exposure-response relationship for vibration induced white finger, *Occupational and Environmental Medicine* 67 (1) (2010) 38–46.
[16] R.G. Dong, J.Z. Wu, D.E. Welcome, T.W. McDowell, Estimation of vibration power absorption density in human fingers, *Journal of Biomechanical Engineering* 127 (5) (2005) 849–856.
[17] L.A. Taber, Biomechanics of growth, remodeling, and morphogenesis, *Applied Mechanics Reviews* 48 (8) (1995) 487–545.
[18] F. Pradko, R. Lee, G. J.D., Human vibration-response theory, *American Society of Mechanical Engineers* (1965), Paper No. 65-WA/HUF-19.
[19] I. Lidstrom, Measurement of energy dissipation by the body when using a vibrating tool, *Nordisk Hygenisk Tidskrift* 2 (1973) 41–45 (in Swedish).
[20] J. Cundiff, Energy dissipation in human hand-arm exposed to random vibration, *Journal of the Acoustical Society of America* 59 (1976) 212–214.
[21] R.G. Dong, D.E. Welcome, T.W. McDowell, J.Z. Wu, A.W. Schopper, Frequency weighting derived from power absorption of fingers-hand-arm system under z(h)-axis vibration, *Journal of Biomechanics* 39 (12) (2006) 2311–2324.
[22] R.G. Dong, J.Z. Wu, D.E. Welcome, T.W. McDowell, A discussion on comparing alternative vibration measures with frequency-weighted accelerations defined in ISO standards, *Journal of Sound and Vibration* 317 (3–5) (2008) 1042–1050.
[23] J.H. Dong, R.G. Dong, S. Rakheja, D.E. Welcome, T.W. McDowell, J.Z. Wu, A method for analyzing absorbed power distribution in the hand and arm substructures when operating vibrating tools, *Journal of Sound and Vibration* 311 (2008) 1286–1309.
[24] B. Buchholz, T.J. Armstrong, An ellipsoidal representation of human hand anthropometry, *Human Factors* 33 (4) (1991) 429–441.
[25] B. Buchholz, T.J. Armstrong, S.A. Goldstein, Anthropometric data for describing the kinematics of the human hand, *Ergonomics* 35 (3) (1992) 261–273.
[26] R. Baran, Nail anatomy and physiology, in: P. Agache, P. Humbert (Eds.), *Measuring the Skin*, Springer-Verlag, Berlin, Heidelberg, 2004, pp. 290–293.
[27] H. Yamada, *Strength of Biological Materials*, Williams and Wilkins Co., Baltimore, 1970.
[28] J.Z. Wu, D.E. Welcome, R.G. Dong, Three-dimensional finite element simulations of the mechanical response of the fingertip to static and dynamic compressions, *Computer Methods in Biomechanics and Biomedical Engineering* 9 (1) (2006) 55–63.
[29] J.Z. Wu, R.G. Dong, D.E. Welcome, Analysis of the point mechanical impedance of fingerpad in vibration, *Medical Engineering & Physics* 28 (8) (2006) 816–826.
[30] E. Concettoni, M. Griffin, The apparent mass and mechanical impedance of the hand and the transmission of vibration to the fingers, hand, and arm, *Journal of Sound Vibration* 325 (3) (2009) 664–678.
[31] D.G. Fertis, *Mechanical and Structural Vibration*, John Wiley and Sons, Inc, New York, Chichester, 1995.
[32] J.Z. Wu, R.G. Dong, W.P. Smutz, Effects of static compression on the vibration modes of a fingertip, *Journal of Low Frequency Noise, Vibration and Active Control* 21 (4) (2002) 229–243.